PHYSICAL REVIEW B VOLUME 52, NUMBER 2 1 JULY 1995-II

Magnetic transitions and nearly reentrant superconducting properties of $HoNi_2B_2C$

M. S. Lin, J. H. Shieh, Y. B. You, W. Y. Guan, and H. C. Ku
Department of Physics, National Tsing Hua University, Hsinchu, Taiwan 300, Republic of China

H. D. Yang
Department of Physics, National Sun Yat-Sen University, Kaohsiung, Taiwan 840, Republic of China

J. C. Ho
Department of Physics and National Institute for Aviation Research, Wichita State University, Wichita, Kansas 67260
(Received 27 February 1995)

A low-temperature phase diagram $H(T)$ of the 7.8-K superconductor $HoNi_2B_2C$ (with an onset of 8.3 K) is generated through characterization of well-prepared samples by various experimental techniques including ac magnetic susceptibility, superconducting quantum interference device dc magnetic susceptibility, magnetic hysteresis, specific heat, and electrical resistivity measurements. The results yield a superconducting upper critical field $H_{c2}(0)$ of 3.5 kG, a lower critical field $H_{c1}(0)$ of 250 G, and a Ginzburg-Landau parameter κ of 3.5. A nearly reentrant deep minimum at 5.2 K with very small H_{c2} of 400 G and H_{c1} of 5 G are observed. Two distinct magnetic transitions are observed with an incommensurate magnetic ordering temperature T_m of 5.7–6 K and an antiferromagnetic Néel temperature T_N of 5.2 K. The magnetic entropy $\Delta(S_m+S_N)$ estimated between 2 and 10 K is 10.4 J/mol K. The effective internal field which causes the nearly reentrant behavior is 2 kG at 5.2 K.

I. INTRODUCTION

Relatively high superconducting transition temperatures T_c up to 23 K have been reported in the quaternary borocarbide RT_2B_2C compounds (R =Sc, Y, Th, U or a rare earth; T=Ni, Pd, or Pt).[1–11] The superconducting phase has been identified to be of the body-centered-tetragonal $LuNi_2B_2C$ type with space group $I4/mmm$. The structure is a three-dimensionally connected framework with LuC layers alternated with Ni_2B_2 layers, where nickel is tetrahedrally coordinated by four boron atoms.[4]

Among many nonmagnetic compounds in the Ni system, $LuNi_2B_2C$ exhibits the highest T_c of 16.6 K, followed by 15–16 K for YNi_2B_2C and metastable $ScNi_2B_2C$,[1,3–8] 7 K for $ThNi_2B_2C$,[8] and no superconducting transition was found down to 2 K for $LaNi_2B_2C$.[8] Band-structure calculations on $LuNi_2B_2C$ (Refs. 12,13) indicate a high density of states $N(E_F)$ at the Fermi level near the top of the almost-filled Ni($3d$) band, with only modest admixture from B and C. All characteristics are indicative of a good, three-dimensional metal. A strong-coupled phonon mechanism for the occurrence of superconductivity is deduced with a very large electron-phonon coupling parameter λ, which is related to an unusual combination of electronic states at the Fermi level and a substantial contribution from the vibration of the light atoms.[12]

For compounds containing magnetic rare earth elements such as R=Dy, Ho, Er, and Tm, lower T_c values were observed due to the magnetic pair-breaking effect.[3] In fact, $HoNi_2B_2C$ is the most intensively studied compound of the Ni-based system due to its nearly reentrant behavior around 5–6 K below the superconducting transition temperature T_c of 7.5–8 K.[6,14–17] However, the reported magnetic transition temperatures are ill defined. For example, while yielding consistently an antiferromagnetic transition temperature T_N around 5 K,[15,16] two neutron diffraction measurements give two different incommensurately modulated/spiral magnetic transition temperatures T_m of 8 K (Ref. 15) and 6 K (Ref. 16), respectively. Meanwhile, prior specific-heat measurements show vaguely two shoulders around 5.5 and 6 K, in addition to a T_N of 5 K. The temperature dependence of superconducting upper critical field $H_{c2}(T)$ is also ambiguous. The zero-temperature value $H_{c2}(0)$ of 4.5 kG, a local minimum at 5.2 K, and a local maximum at 6.2 K were obtained from field-dependent electrical resistivity measurements[6] in contrast to 1.9 kG, 5–5.2 K, and 6 K, respectively, from magnetic measurements on a single crystal.[14]

In this work, we have characterized a well-prepared $HoNi_2B_2C$ polycrystalline sample through various experimental techniques including ac magnetic susceptibility, superconducting quantum interference device (SQUID) dc magnetic susceptibility, magnetic hysteresis, specific-heat, and electrical resistivity measurements. A phase diagram of this quaternary compound is thus generated with reference to the temperature dependence of critical magnetic fields.

II. EXPERIMENTS

$HoNi_2B_2C$ samples were prepared from high-purity elements Ho (99.9%, ingot), Ni (99.9% foil), B (99.9995% chips), and C (99.995% chips) with a stoichiometric ratio

0163-1829/95/52(2)/1181(6)/$06.00

of (1:2:2:1) under an argon atmosphere in a Zr-gettered arc furnace. The Ho, B, and C ingredients were wrapped in the Ni foil and arc melted carefully several times to ensure negligible weight loss and sample homogeneity. The as-melted samples were then wrapped in Ta foils and annealed under argon atmosphere in a sealed quartz tube at 1100 °C for three days and then quenched in liquid nitrogen. Crystallographic data were obtained with a Rigaku Rotaflex 18-kW rotating anode powder x-ray diffractometer using Cu $K\alpha$ radiation with a scanning rate of 1° in 2θ per min. A LAZY PULVERIX PC program was employed for phase identification and lattice parameter calculation.

Electrical resistivity measurements (16 Hz) were carried out by the standard four-probe method in an RMC Cryosystems closed-cycle refrigerator down to 9 K and using single-shot cooling to 6.5 K. ac magnetic susceptibility measurements were made with a Lake Shore Model 7221 susceptometer/magnetometer down to 4.2 K in an ac magnetic field 0.1 or 0.01 G (rms) at 1 kHz. The ac signal can be biased by a dc magnetic field up to 1 T. dc magnetic susceptibility and magnetic hysteresis measurements were made with a Quantum Design MPMS or a Mu-metal shielded $MPMS_2$ SQUID magnetometer down to 2 K in an applied field from 1 G to 1 T. Specific-heat measurements were made with an adiabatic calorimeter from 1.5 to 20 K. The sample was thermally anchored to a copper block containing a germanium thermometer and a manganin wire heater, for which measurements were made separately for addenda correction.

III. RESULTS AND DISCUSSION

In preparing $HoNi_2B_2C$ samples, a minute amount of Ni_2B impurity often prevails,[18] which can actually serve as the flux in growing $HoNi_2B_2C$ single crystals.[14] For the annealed samples used in this work, the powder x-ray diffraction pattern in Fig. 1 reflects practically a single phase. The diffraction lines can be well indexed with the $LuNi_2B_2C$-type structure having tetragonal lattice parameters $a = 3.516(3)$ Å, $c = 10.530(6)$ Å, and unit cell volume $V = 130.2(1)$ Å^3. The excellent sample quality is attributed to the use of Ni foil as the wrap of the high-purity starting materials, followed by liquid nitrogen quench after annealing.

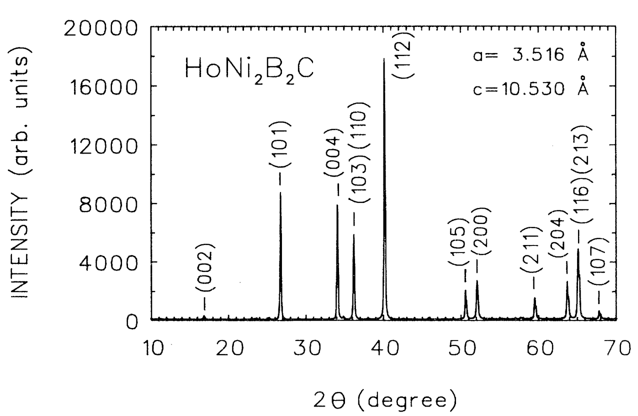

FIG. 1. Powder x-ray diffraction pattern of annealed $HoNi_2B_2C$ sample.

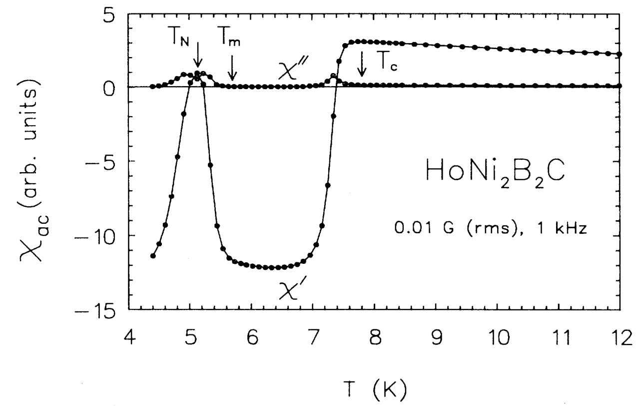

FIG. 2. Low-temperature real and imaginary parts of ac magnetic susceptibilities $\chi_{ac}(T)=\chi'(T)+i\chi''(T)$ (0.01 G rms at 1 kHz) for bulk sample. Three distinct transitions were observed.

A. Superconducting and magnetic transitions

The low-temperature real and imaginary parts of ac magnetic susceptibilities $\chi_{ac}(T)=\chi'(T)+i\chi''(T)$ of the annealed $HoNi_2B_2C$ bulk sample are shown together in Fig. 2, with 0.01 G (rms) ac field at 1 kHz frequency. Three phase transitions around 7.8, 5.7, and 5.2 K can be identified from the imaginary part. The first one at 7.8 K corresponds to a superconducting transition as the transition is accompanied by a diamagnetic, superconducting real part signal. This is consistent with the transport data in Fig. 3, where the temperature dependence of electrical resistivity $\rho(T)$ shows a superconducting transition with 10% resistivity onset drop T_c (onset) of 8.3 K, 50% midpoint drop T_c (mid) of 8.1 K, and zero resistivity T_c (zero) of 7.8 K. The small extrapolated residual resistivity ρ(0 K) of 24 $\mu\Omega$ cm, along with the large metallic resistivity ratio $\rho(RT)/\rho(9\ K)$ of 7.5, are indications of good polycrystalline sample quality. The $T_c = 7.8$ K for

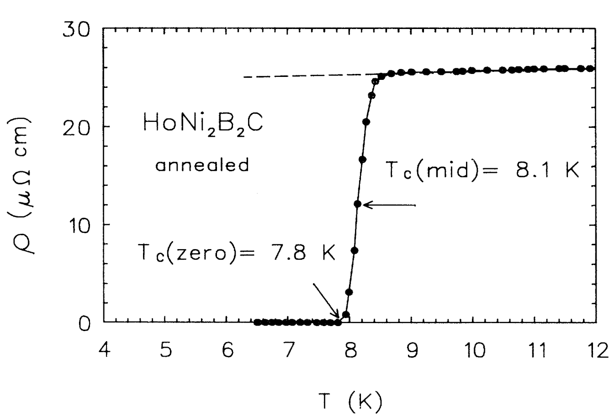

FIG. 3. Low-temperature electrical resistivity $\rho(T)$.

$HoNi_2B_2C$ is 8.8 K lower than the $T_c = 16.6$ K for nonmagnetic $LuNi_2B_2C$. Judging from the systematic variation of T_c with Ni-Ni in-plane distance $d = a/\sqrt{2}$ (a is the tetragonal lattice parameter) for the nonmagnetic compounds RNi_2B_2C (R=Sc, Lu, Y, Th, or La),[8] the T_c depression due to the magnetic pair-breaking effect at $d = 2.468$ Å (for $HoNi_2B_2C$ with $a = 3.516$ Å) can be estimated as $\Delta T_c(\text{Ho}) = T_{c0}(\text{Ho}) - T_c(\text{Ho}) = 15.8$ K$-$7.8 K$=$8 K,[8] or about 90% of the observed T_c depression as compared with $LuNi_2B_2C$. If the magnetic pair-breaking effect is in the framework of the Abrikosov-Gor'kov theory with ΔT_c proportional to the de Gennes factor $(g_J - 1)^2 J(J+1)$, where J is the total angular momentum and g_J is the Landé g-factor,[19] then using $\Delta T_c(\text{Ho}) = 8$ K and the calculated Fermi-level density of states $N(E_F)$ of 4.8 states/eV cell or 0.8 states/eV atom for $LuNi_2B_2C$,[13] a small exchange-coupling parameter $|J|$ of 8.1 meV between conduction electron and localized $4f$ moment is derived by using the formula $\Delta T_c = [\pi^2 N(E_F)/6 \times 2k_B]|J|^2 (g_J - 1)^2 J(J+1)$. The tetragonal crystal-field effect (CEF) is neglected for the present crude estimation. The same $T_c(d)$ curve with $\Delta T_c / T_{c0}$ proportional to the de Gennes factor can also be used to predict the superconducting transition temperature of $DyNi_2B_2C$ using T_{c0} (Dy) of 15.3 K at $d = 2.498$ Å (for $DyNi_2B_2C$ with $a = 3.532$ Å).[8,20] The calculated $T_c(\text{Dy}) = 3.1$ K is indeed close to T_c of 3.8 K observed in our preliminary study[20] and is higher than the previously reported T_c onset around 2 K.[6]

The two other transitions observed at 5.7 and 5.2 K from ac magnetic susceptibility data are apparently related to the long-range Ho^{3+} magnetic ordering through the Ruderman-Kittel-Kasuya-Yosida indirect exchange interaction. The real part ac signal indicates a nearly reentrant behavior starting from the magnetic ordering temperature T_m around 5.7 K, reaching to a small positive peak at the antiferromagnetic Néel temperature T_N of 5.2 K, then dropping sharply back to diamagnetic signal below T_N.[17] No nearly reentrant behavior can be detected from the resistivity measurement due to the low-temperature limit of 6.5 K. However, these two magnetic transitions can be clearly corroborated by low-temperature specific-heat data $C(T)$ as shown in Fig. 4. Two distinct transition peaks were observed at 5.7 and 5.2 K, respectively. The expected specific-heat discontinuity at T_c would be of the order of mJ/mol K, and is too small to be observed in the presence of large magnetic contributions. Strictly speaking, there should be four contributions to the total heat capacity $C = \gamma T + \beta T^3 + C_m + C_N$, corresponding to the electronic, the lattice, and the two magnetic transition components, respectively. By employing the literature data for nonmagnetic $LuNi_2B_2C$ (Ref. 21) as the base line representing the electronic and lattice terms, the magnetic entropy between 2 and 10 K can be derived as $\Delta(S_m + S_N) = \int [(C - 0.019T - 0.00035T^3)/T] dT = 10.4$ J/mol K. Additional contributions to the magnetic entropy below 2 K and above 10 K are relatively insignificant, judging from the data in Fig. 4. The small difference between 10.4 J/mol K and $S_N = R \ln 3 = 9.12$ J/mol K, which is expected for the antiferromagnetic ordering of Ho^{3+} with a quasitriplet ground state (closely spaced doublet and singlet levels) in the tetragonal crystal field,[14] could simply be the consequence of the change-over from an antiferromagnetic state to the incommensurate modulated/spiral magnetic structure near T_m. Such a transition should be considered as an order-to-order process with a latent heat. In fact, the minor peak at $T_m = 5.7$ K can easily account for such a ΔS_m value. More importantly, the magnetic transition temperatures are consistent with the results of single-crystal neutron diffraction measurements,[16] where a simple commensurate antiferromagnetic structure was observed with moments aligned in the tetragonal basal plane around 5 K and an incommensurate modulated/spiral magnetic transition was developed around 6 K with the ferromagnetic planes rotating from layer to layer along the c axis with a turn angle of 165°, and the neighboring moments along the a axis are rotated by approximately 104°.[16] The persistence of the neutron satellite peaks up to 8 K from the powder neutron data may be due to the strong short-range magnetic fluctuation.[15]

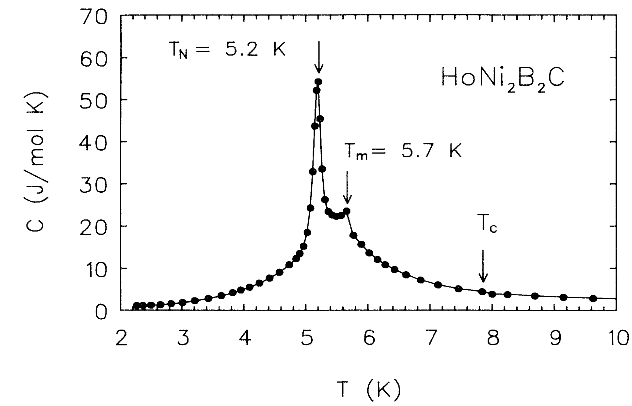

FIG. 4. Temperature dependence of specific heat $C(T)$. Two distinct magnetic transitions were observed.

Identical results are obtained from the low-field (1 G), zero-field-cooled (ZFC), and field-cooled (FC) dc mass magnetic susceptibilities $\chi_g(T)$ as shown in Fig. 5. A powder sample with fine particle size of around 1 μm is used to avoid any unwanted shielding signal and the complex flux-pinning effect which are always observed for bulk borocarbide samples. The superconducting transition temperature T_c of 7.8 K was observed from the merging point of the ZFC and FC curves, which is also the onset deviation from the Curie-Weiss law, with a large ZFC signal of -1.3×10^{-2} emu/g G and FC signal of -7.1×10^{-3} emu/g G at 2 K. Using x-ray density of 4.02 g/cm^3, volume susceptibility percentages $4\pi\chi$ of 66% (ZFC) and 36% (FC) at 2 K are obtained for the powder sample, indicating good sample quality. Nearly reentrant behavior is also observed with a T_N peak of 5.2 K and T_m upturn around 6 K. The large positive χ_g value of 3.3×10^{-3} emu/g G at 5.2 K is still smaller than 4.1×10^{-3} emu/g G at T_c of 7.8 K.

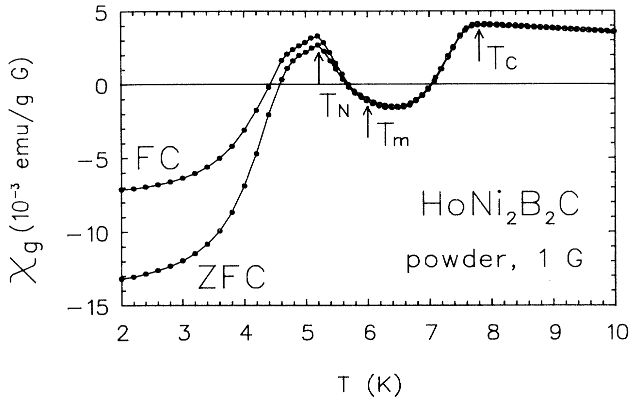

FIG. 5. Low-temperature, low-field (1 G) dc mass magnetic susceptibility $\chi_g(T)$ for powder sample, measured in both field-cooled (FC) and zero-field-cooled (ZFC) modes.

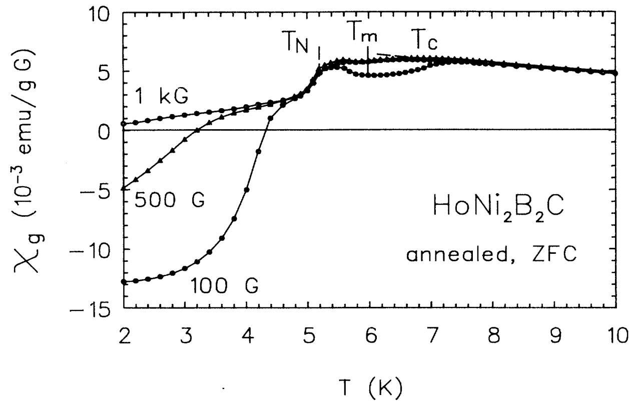

FIG. 7. Low-temperature zero-field-cooled (ZFC) dc mass magnetic susceptibility $\chi_g(T)$ (100, 500, and 1 kG) for bulk samples.

B. Superconducting upper critical field $H_{c2}(T)$ and lower critical field $H_{c1}(T)$

Several methods are used to determine the superconducting upper critical field $H_{c2}(T)$ and lower critical field $H_{c1}(T)$.

The low-temperature ac magnetic susceptibility $\chi_{ac}(T)$ in ac field of 0.1 G (rms) at 1 kHz with a dc-biased magnetic field of 100 G is shown in Fig. 6. T_c decreases from 7.8 K in the zero-field-biased case to 7.5 K in the 100-G-biased case, or $H_{c2}(7.5\ K)=100$ G. T_m of 6 K and T_N of 5.2 K are observed. A small bump around 4.5 K was observed below T_N. Judging from the shape of the real part signal, these magnetic structures under applied field may be slightly weakly ferromagnetic.

The field-dependent low-temperature ZFC dc mass magnetic susceptibilities $\chi_g(T)$ in various applied fields of 100, 500, and 1 kG for bulk samples are shown collectively in Fig. 7. T_c decreases from 7.8 K in 1 G to 7.5 K in 100 G, 6.8 K in 500 G, and 6.5 K in 1 kG applied field. T_m and T_N are almost field independent in these low applied fields. The small bump observed in ac magnetic susceptibility is reflected as a knee at 4.5 K for $\chi_g(T)$ in 100 G applied field. This bump is suppressed to 3.5 K in 500 G and is no longer observable in 1 kG. Superconductivity is completely destroyed in 5 kG as shown in Fig. 8, where only the two unchanged magnetic transitions of T_m and T_N remain.

Constant-temperature magnetic hysteresis measurements provide more precise information on the temperature dependence of superconducting upper critical field $H_{c2}(T)$. As in Fig. 9, a $H_{c2}(T)$ value of 3 kG for 2 K is determined from the merging point of the hysteresis curve as indicated by the arrow. Similarly, H_{c2} is 1 kG at 4 K. Moreover, each $M(H)$ curve has a linear, nonhysteretic, paramagneticlike background due to simple commensurate antiferromagnetic structure with moments aligned in the tetragonal basal plane.[15,16] The exchange interaction is ferromagnetic in the basal plane with weak antiferromagnetic coupling mediated through the Ni layers.

Figure 10 yields higher-temperature H_{c2} values of 400 G at 5.2 K (T_N) and 300 G at 7 K ($>T_m$). Finally, it is of particular interest to note that, more than the superconducting hysteretic behavior at 6 K (near T_m), a non-

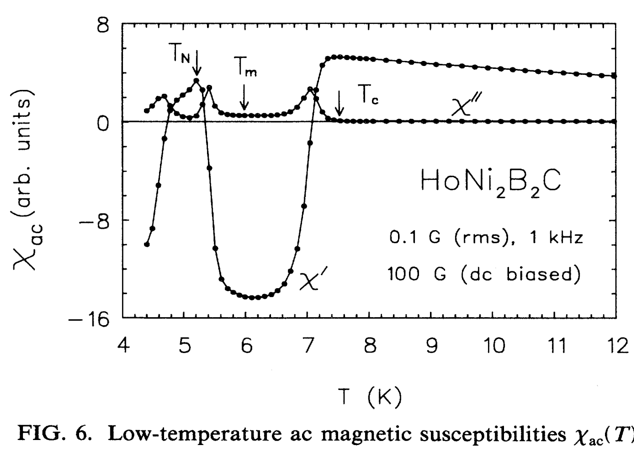

FIG. 6. Low-temperature ac magnetic susceptibilities $\chi_{ac}(T)$ (0.1 G rms at 1 kHz) in a dc-biased field of 100 G.

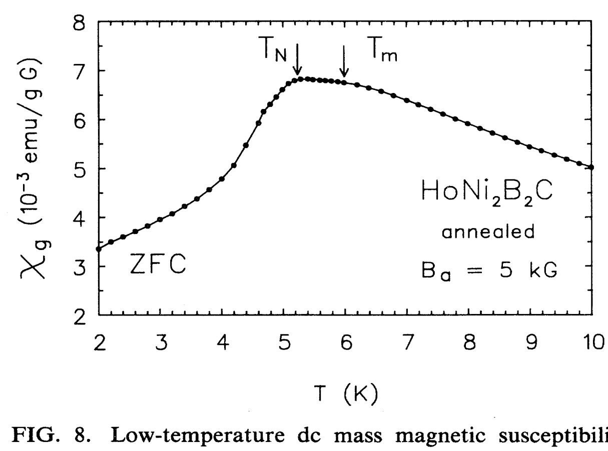

FIG. 8. Low-temperature dc mass magnetic susceptibility $\chi_g(T)$ in a higher field of 5 kG.

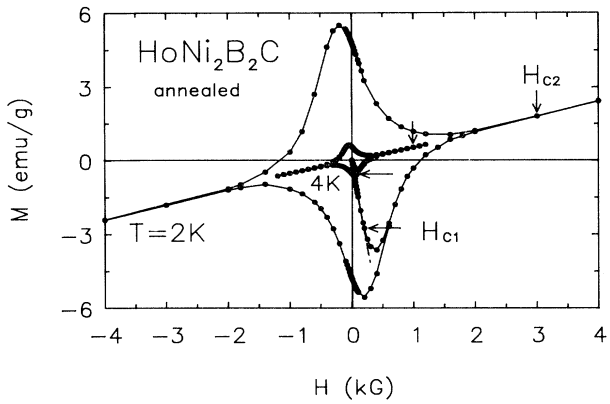

FIG. 9. Magnetic hysteresis curves $M(H)$ at 2 and 4 K ($<T_N$). Upper critical field H_{c2} and lower critical field H_{c1} are indicated by arrows.

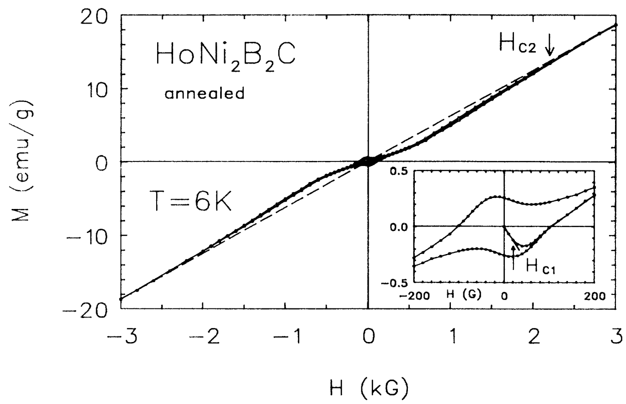

FIG. 11. Magnetic hysteresis curves $M(H)$ at 6 K ($\sim T_m$).

linear magnetic background was present in Fig. 11. Meanwhile, a much enhanced H_{c2} of 2.2 kG was obtained at this temperature. This complex background is apparently due to the onset of the incommensurate modulated/spiral magnetic structure.

The temperature dependence of superconducting lower critical field $H_{c1}(T)$ can also be determined from the magnetic hysteresis measurements as shown in Figs. 9–11. The $H_{c1}(T)$ is defined as the deviation from linearity in the initial magnetization in each $M(H)$ curve in Figs. 9–11. The values thus obtained are 10 G at 7 K, 20 G at 6 K, 5 G at 5.2 K, 50 G at 4 K, and 200 G at 2 K.

C. Low-temperature phase diagram

Based on this work and the data analysis outlined above, the low-temperature phase diagram $H(T)$ of $HoNi_2B_2C$ is generated and given in Fig. 12. In terms of the temperature dependence of critical fields, the extrapolated $H_{c2}(0)$ value is 3.5 ± 0.5 kG while the extrapolated upper limit of $H_{c1}(0)$ is 250 ± 100 G. The previously reported $H_{c2}(0)$ value of 1.9 kG from single-crystal magnetic data[14] is apparently too low since a $H_{c2}(2\text{ K})$ value of at least 3.0 kG was already observed experimentally from the hysteresis measurement. On the other hand, the $H_{c2}(0)$ value of 3.5 kG is less than 4.5 kG reported from resistivity data where the H_{c2} values are arbitrarily defined as the midpoint resistivity drop.[6] The resistivity data may yield the surface critical field H_{c3}, which is the limit of field in which superconductivity can persist at the surface of the sample,[22] rather than H_{c2}.

From $H_{c1}(0)$ and $H_{c2}(0)$, the Ginzburg-Landau parameter κ value of 3.5 is evaluated using the formula $H_{c2}/H_{c1}=2\kappa^2/(\ln\kappa+0.5)$.[23] As a comparison, κ values of 12–15 are reported for nonmagnetic, higher-T_c YNi_2B_2C and $LuNi_2B_2C$.[24,25] From the local minimum of 400 G at T_N of 5.2 K and the shape of the $H_{c2}(T)$ curve, a maximum effective internal field H_{int} of 2 kG is deduced. The relatively slow recovery of $H_{c2}(T)$ below T_N may be due to the incommensurate magnetic fluctuation where the neutron data indicate that the fluctuation is persisted down to lower temperatures.[15,16]

The phase diagram with two magnetic transitions below T_c reported for $HoNi_2B_2C$ is indeed very similar to the previously reported pseudoternary $Ho(Rh_{1-x}Ir_x)_4B_4$

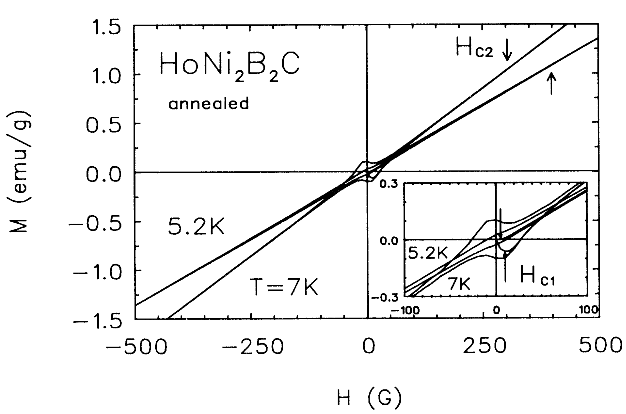

FIG. 10. Magnetic hysteresis curves $M(H)$ at 5.2 K (T_N) and 7 K ($>T_m$).

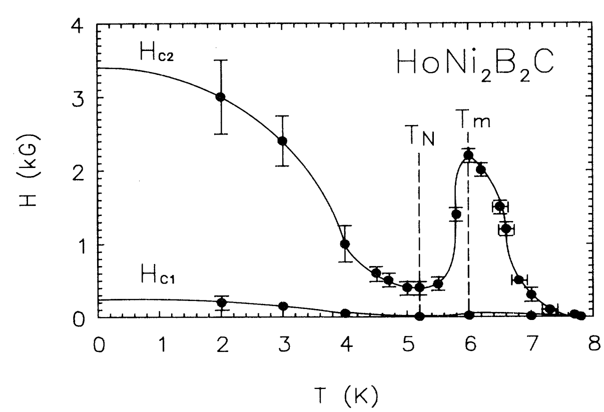

FIG. 12. Low-temperature phase diagram $H(T)$ (T_m, T_N, H_{c2}, and H_{c1}) for $HoNi_2B_2C$. The solid and dashed lines are for guiding the eyes only.

system[26–28] with compositions around $0.25 < x < 0.5$. For example, the $Ho(Rh_{0.7}Ir_{0.3})_4B_4$ compound is superconducting at 5.5 K with two distinct magnetic transitions at 1.12 and 0.86 K from the specific-heat data. Nearly reentrant behavior is expected between these two magnetic transitions. True reentrant behavior was indeed observed for $0.075 < x < 0.25$. For example, superconductivity of 5.2 K $Ho(Rh_{0.85}Ir_{0.15})_4B_4$ was completely destroyed by a ferromagnetic ordering with Curie temperature T_C at 2.77 K.

IV. CONCLUSION

Well-prepared $HoNi_2B_2C$ samples were characterized by various experimental techniques including ac magnetic susceptibility, SQUID dc magnetic susceptibility, magnetic hysteresis, specific-heat, and electrical resistivity measurements. The results yield three distinct phase transitions: a superconducting transition temperature T_c of 7.8 K (with onset of 8.3 K), and incommensurate magnetic ordering temperature T_m of 5.7–6 K, and an antiferromagnetic Néel temperature T_N of 5.2 K. Furthermore, a low-temperature phase diagram of this nearly reentrant magnetic superconductor is generated in terms of temperature dependence of H_{c1}, H_{c2}, T_m, and T_N. From the extrapolated H_{c1} (0) of 250±100 G and $H_{c2}(0)$ of 3.5±0.5 kG, the Ginzburg-Landau parameter κ value of 3.5 is derived.

ACKNOWLEDGMENT

This work was supported by the National Science Council of the Republic of China under Contract Nos. NSC84-2112-M007-003 and -038.

[1]R. Nagarajan, C. Mazumdar, Z. Hossain, S. K. Dhar, K. V. Gopalakrishnan, L. C. Gupta, C. Godart, B. D. Padalia, and R. Vijayaraghavan, Phys. Rev. Lett. **72**, 274 (1994).

[2]R. J. Cava, H. Takagi, B. Batlogg, H. W. Zandbergen, J. J. Krajewski, W. F. Peck, Jr., R. B. van Dover, R. J. Felder, T. Siegrist, K. Mizuhashi, J. O. Lee, H. Eisaki, S. A. Carter, and S. Uchida, Nature **367**, 146 (1994).

[3]R. J. Cava, H. Takagi, H. W. Zandbergen, J. J. Krajewski, W. F. Peck, Jr., T. Siegrist, B. Batlogg, R. B. van Dover, R. J. Felder, K. Mizuhashi, J. O. Lee, H. Eisaki, and S. Uchida, Nature **367**, 252 (1994).

[4]T. Siegrist, H. W. Zandbergen, R. J. Cava, J. J. Krajewski, and W. F. Peck, Jr., Nature **367**, 254 (1994).

[5]H. C. Ku, C. C. Lai, Y. B. You, J. H. Shieh, and W. Y. Guan, Phys. Rev. B **50**, 351 (1994).

[6]H. Eisaki, H. Takagi, R. J. Cava, B. Batlogg, J. J. Krajewski, W. F. Peck, Jr., K. Mizuhashi, J. O. Lee, and S. Uchida, Phys. Rev. B **50**, 647 (1994).

[7]J. L. Sarrao, M. C. de Andrade, J. Herrmann, S. H. Han, Z. Fisk, M. B. Maple, and R. J. Cava, Physica C **229**, 65 (1994).

[8]C. C. Lai, M. S. Lin, Y. B. You, and H. C. Ku, Phys. Rev. B **51**, 420 (1995).

[9]Z. Hossain, L. C. Gupta, C. Mazumdar, R. Nagarajan, S. K. Dhar, C. Godart, C. Levy-Clement, B. D. Padalia, and R. Vijayaraghavan, Solid State Commun. **92**, 341 (1994).

[10]R. J. Cava, B. Batlogg, T. Siegrist, J. J. Krajewski, W. F. Peck, Jr., S. Carter, R. J. Felder, H. Takagi, and R. B. van Dover, Phys. Rev. B **49**, 12 384 (1994).

[11]P. J. Jiang, M. S. Lin, J. H. Shieh, Y. B. You, H. C. Ku, and J. C. Ho, Phys. Rev. B **51**, 16 436 (1995).

[12]L. F. Mattheiss, Phys. Rev. B **49**, 13 279 (1994).

[13]W. E. Pickett and D. J. Singh, Phys. Rev. Lett. **72**, 3702 (1994).

[14]P. C. Canfield, B. K. Cho, D. C. Johnston, D. K. Finnemore, and M. F. Handley, Physica C **230**, 397 (1994).

[15]T. E. Grigereit, J. W. Lynn, Q. Huang, A. Santoro, R. J. Cava, J. J. Krajewski, and W. F. Peck, Jr., Phys. Rev. Lett. **73**, 2756 (1994).

[16]A. I. Goldman, C. Strassis, P. C. Canfield, J. Zaretsky, P. Dervenagas, B. K. Cho, D. C. Johnston, and B. Sternlieb, Phys. Rev. B **50**, 9668 (1994).

[17]H. Schmidt and H. F. Braun, Physica C **229**, 315 (1994).

[18]E. E. Havinga, H. Samasma, and P. Hokkeling, J. Less-Common Met. **27**, 169 (1972); **27**, 281 (1972). No superconducting transition down to 0.07 K was reported for Ni_2B phase.

[19]A. A. Abrikosov and L. P. Gor'kov, Sov. Phys. JETP **12**, 1243 (1961).

[20]M. S. Lin and H. C. Ku, Physica C (to be published).

[21]S. A. Carter, B. Batlogg, R. J. Cava, J. J. Krajewski, W. F. Peck, Jr., and H. Takagi, Phys. Rev. B **50**, 4216 (1994).

[22]D. Saint-James and P. G. deGennes, Phys. Lett. **7**, 306 (1963).

[23]C. R. Hu, Phys. Rev. B **6**, 1756 (1972).

[24]M. Xu, P. C. Canfield, J. E. Ostenson, D. K. Finnemore, B. K. Cho, Z. R. Wang, and D. C. Johnston, Physica C **227**, 321 (1994).

[25]H. Takagi, R. J. Cava, H. Eisaki, J. O. Lee, K. Mizuhashi, B. Batlogg, S. Uchida, J. J. Krajewski, and W. F. Peck, Jr., Physica C **228**, 389 (1994).

[26]H. C. Ku, F. Acker, and B. T. Matthias, Phys. Lett. **76A**, 399 (1980).

[27]K. N. Yang, S. E. Lambert, H. C. Hamaker, M. B. Maple, H. A. Mook, and H. C. Ku, in *Superconductivity in d- and f-Band Metals,* edited by W. Buckel and W. Weber (Kernforschungszentrum, Karlsruhe, 1982), p. 217.

[28]H. C. Ku, P. Klavins and R. N. Shelton, Physica B **148**, 117 (1987).